Electronic structure of carbon-free silicon oxynitride films grown using an organic precursor hexamethyl-disilazane

2002 J. Phys. D: Appl. Phys. 35 L44

(http://iopscience.iop.org/0022-3727/35/11/103)

INSTITUTE OF PHYSICS PUBLISHING JOURNAL OF PHYSICS D: APPLIED PHYSICS
J. Phys. D: Appl. Phys. **35** (2002) L44–L47 PII: S0022-3727(02)34668-0

RAPID COMMUNICATION

Electronic structure of carbon-free silicon oxynitride films grown using an organic precursor hexamethyl-disilazane

A Chainani, S K Nema, P Kikani and P I John

Institute for Plasma Research, Gandhinagar 382 428, Gujarat, India

Received 8 March 2002
Published 21 May 2002
Online at stacks.iop.org/JPhysD/35/L44

Abstract
Silicon oxynitride films are grown by plasma-enhanced chemical vapour deposition on single-crystal Si(100) and textured Si solar cells, using a safe organic precursor, hexamethyl-disilazane. Using the Lucovsky–Phillips criterion of bond coordination constraints, we grow high-quality thin (∼20 Å) and thick (up to 2700 Å) films which are carbon free (<1.0%) as characterized by x-ray photoemission spectroscopy (XPS) and Auger electron spectroscopy depth profiles. Core-level and valence band XPS is used to conclusively identify oxynitride bonding and band gap reduction in SiO_xN_y. For a $\lambda/4$ 'blue' anti-reflection coating on the solar cells with uniform thickness (870 ± 15 Å) and composition ($SiO_{1.6\pm0.1}N_{0.3\pm0.05}$), an efficiency (AM 1) increase of 1% is obtained.

The study of silicon oxynitride (SiO_xN_y) films continues to be very important in MOS device technology [1] and in optical applications [2]. In particular, the improved I–V and C–V characteristics, and higher dielectric breakdown values are directly ascribed to the role of nitrogen in oxynitride films. Nitridation of thin SiO_2 films decreases interface state generation [3], and results in reduced low field leakage current and boron diffusion from the substrate [4, 5]. While ultrathin films are required for ULSI technology, relatively thick SiO_xN_y films are used to make optical devices such as low-pass, high-pass and band-pass filters which select a part of the transmitted or reflected light and are thus useful as anti-reflection (AR) coatings, thermal control coatings, decorative coatings as well as for optical communication waveguides [2]. It is now also possible to make SiO_xN_y multilayer filters and the so-called rugate filters, in which the refractive index varies periodically as a function of thickness [6].

SiO_xN_y can be grown by a variety of methods: heating a bare silicon wafer in N_2O/NO at high temperatures (∼1000°C) in a conventional furnace or by rapid thermal annealing (RTA), low-pressure CVD at 875°C or low temperature (<300°C) PECVD using silane (SiH_4), plasma nitridation of SiO_2 films using N_2O, NO or NH_3, etc. Using high-resolution chemical etching and secondary ion mass spectroscopy/ion scattering spectroscopy, nitrogen accumulation at the Si/SiO_2 interface due to RTA has been identified, while conventional furnace annealing gives a uniform nitrogen distribution throughout the film thickness [4, 7]. The nitrogen content and its distribution as a function of depth, as well as its detailed bonding structure, depend on the process employed and are being intensively studied in order to tailor device properties [1, 8–10]. In spite of difficulties in handling SiH_4, work on SiO_xN_y films has relied on SiH_4 as the preferred source of Si compared to organic precursors. This is because early work using hexamethyl-disiloxane (HMDSO) and hexamethyl-disilazane (HMDSN) resulted in substantial carbon contamination in the films which degrades the properties of the films [11].

In this paper, we study SiO_xN_y films grown by PECVD on single-crystal p-type Si(100) and textured Si solar cells. We grow SiO_xN_y films using a safe organo-silicon precursor, HMDSN: $(CH_3)_6Si_2NH$. Using the criterion of bond coordination constraints established by Lucovsky and Phillips [1], we grow SiO_xN_y films corresponding to an average bond coordination $N_{av} < 3$. It is known that SiO_2 exhibits a $N_{av} \sim 2.67$ which systematically increases to a $N_{av} \sim 3.5$ for Si_3N_4. $N_{av} \sim 3$ separates device quality films from defective interfaces [1]. The elemental composition of the films was

determined using XPS and AES depth profiles and could be varied between $SiO_{1.9}N_{0.1}$ to $SiO_{1.6}N_{0.3}$. Core-level XPS is used to identify the bonding structure in the films. Valence band spectroscopy confirms band gap reduction in SiO_xN_y films compared to SiO_2. The same method is used to grow $SiO_{1.6}N_{0.3}$ films with a thickness of 870 ± 15 Å as an AR coating for textured Si solar cells. An improvement of 1% in the efficiency (AM 1) of solar cells is obtained due to the coating.

SiO_xN_y films were grown on p-type single-crystal Si (100) (resistivity 0.01–0.05 Ω cm) and textured Si solar cells obtained from BHEL, Electronics Division. The PECVD reactor uses a turbo pump, mass flow controllers, and a RF source (13.56 MHz) with a matching network. Following an initial *ex situ* cleaning, the wafers were subjected to an *in situ* cleaning using an Ar gas discharge before carrying out PECVD with wafers placed on the live electrode. Relative concentrations of oxygen and nitrogen in the films was controlled by varying N_2 flow rate between 25 and 50 sccm at a fixed flow rate of 50 sccm of HMDSN. The vaporized HMDSN (Fluka make, containing 1.5% water vapour as source of oxygen) was mixed with N_2 gas prior to introduction into the plasma via a shower head which formed one plate of the capacitive glow discharge. The present variation in N_2 flow rates corresponds to a variation in $O_2/(O_2 + N_2)$ ratio of about 0.03–0.06 as reported earlier [6] for SiO_xN_y films grown using SiH_4. The depositions were carried out at a substrate temperature of 120°C as depositions at higher temperature result in carbon contamination in the films [11]. The resulting films deposited on Si(100) were amorphous as confirmed by absence of diffraction peaks using grazing incidence x-ray diffraction. XPS and small-spot ($\sim 1\,\mu$m) electron-induced AES measurements were carried out in a Multitechnique Physical Electronics System 5702 (USA). XPS and AES studies were done at a vacuum of 8×10^{-10} Torr with the pressure rising to 6×10^{-9} Torr during etching. XPS was carried out using MgKα ($\Delta E = 0.9$ eV) and monochromatic AlKα source ($\Delta E = 0.5$ eV). AES was carried out using an electron gun at a primary energy of 5 keV with a FWHM of 4.2 eV. A depth profile of a thermally grown 1000 Å Ta_2O_5 film was used to calibrate the thickness of the SiO_xN_y films.

In figures 1(*a*)–(*d*), we plot the differential AES spectra of Si LVV, C KVV, O KVV and N KVV obtained for a SiO_xN_y film deposited on a p-type single-crystal Si(100) wafer. The spectra were obtained after half-minute steps of etching and for a total etch time of 10 min (marked 0–5–10, in figures 1(*a*)–(*d*)). In figure 1(*a*), the spectra initially exhibit a broad weak dip feature centred at about 78.5 eV kinetic energy (KE) typical of the Si LVV signal of an oxynitride surface [12]. With increasing etching, the broad feature at 78.5 eV develops a dip at higher KE and transforms into the Si LVV signal of elemental Si at 90 eV. The crossover region is plotted as thick lines in figure 1(*a*). We thus have three regions as a function of etching time or depth from the surface: the deposited film, the crossover/interfacial region and the Si substrate. Throughout the thickness of the film and interfacial region (see figure 1(*b*)), we measure negligible carbon content (<1%, which is the sensitivity of AES). The spectrum obtained without etching (labelled 0 in figure 1(*b*)), however, indicates a carbon content of 8% due to adsorbed species on the surface. XPS measurements were used to confirm that the adsorbed

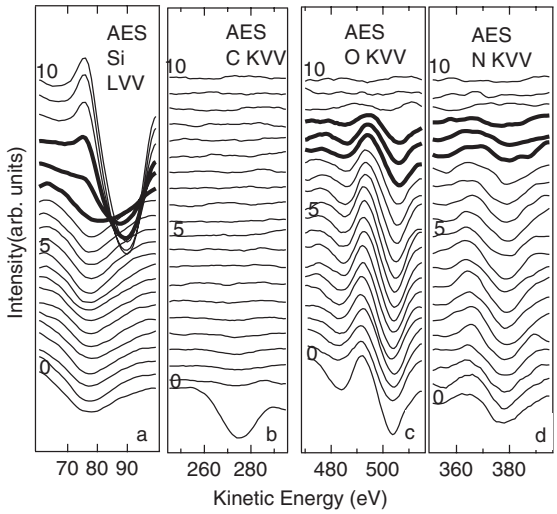

Figure 1. Differential AES spectra using a primary energy of 5 keV for the (*a*) Si LVV, (*b*) C KVV, (*c*) O KVV and (*d*) N KVV levels for SiO_xN_y as a function of etch time (0–5–10 min).

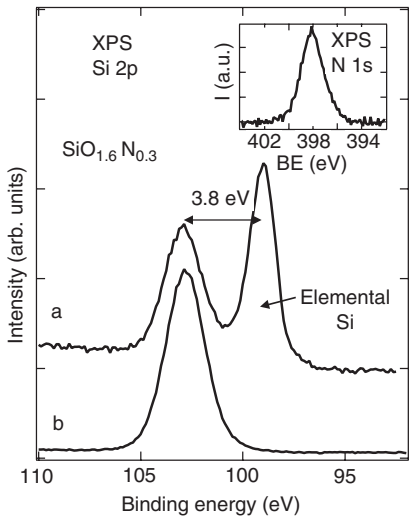

Figure 2. The Si 2p core-level XPS for (*a*) a thin film and (*b*) a thick film of $SiO_{1.6}N_{0.3}$ grown using the same conditions. Inset shows the N 1s spectrum of $SiO_{1.6}N_{0.3}$.

C was reduced to <0.6% after an etch of ~5 Å. Figures 1(*c*) and (*d*) show the O KVV and N KVV AES spectra indicating the same thickness of the film as the Si LVV signal. Using the atomic sensitivity factors for the measured levels [13] we estimate a composition of $SiO_{1.6\pm0.1}N_{0.3\pm0.05}$ for the film.

In figure 2 we plot the Si 2p core level obtained using XPS for (*a*) a thin film of $SiO_{1.6}N_{0.3}$ in comparison with (*b*) a thick film grown using the same conditions. The thin film surface shows elemental Si 2p of the substrate and Si 2p of the oxynitride, the thickness being about 20 Å [14, 15]. The binding energy (BE) of the oxynitride Si 2p is measured to be 102.8 ± 0.1 eV in the thin and thick films while that of elemental Si 2p is 99.0 ± 0.1 eV, as obtained from a curve-fitting analysis of the data. It is known that the BE of elemental Si 2p and that of a thin SiO_2 film on Si exhibit a separation of 4.4 ± 0.1 eV [15]. For the present case of $SiO_{1.6}N_{0.3}$, a reduced separation of 3.8 eV is indicative of an oxynitride; a systematic shift in the Si 2p level from a value of 103.5 ± 0.2 eV

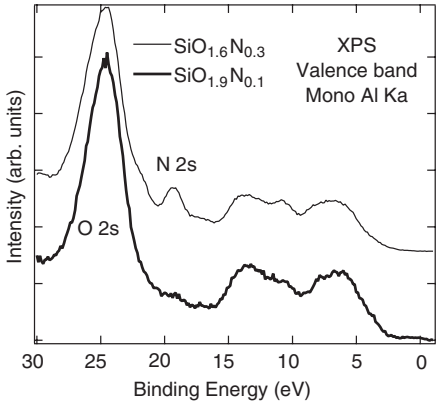

Figure 3. XPS valence band spectra for $SiO_{1.9}N_{0.1}$ and $SiO_{1.6}N_{0.3}$ obtained using a monochromatic Al Kα source.

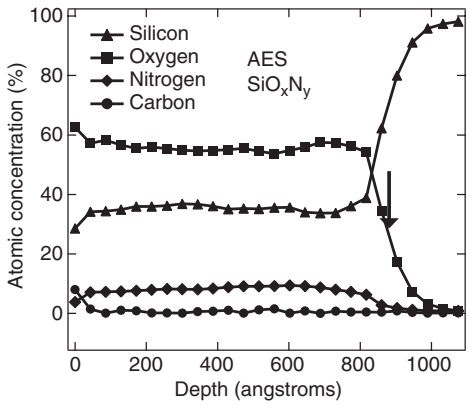

Figure 4. Atomic concentration depth profile for a film of $SiO_{1.6\pm0.1}N_{0.3\pm0.05}$ grown using PECVD. Arrow indicates film thickness of 870 ± 15 Å.

for SiO_2 to 101.9 ± 0.2 eV for Si_3N_4 is well known [13, 16]. The inset in figure 2 shows the N 1s core-level XPS for the deposited film exhibiting a single peak at 398.1±0.1 eV. This is typical of the N 1s of an oxynitride film grown using SiH_4 and N_2O/NH_3 with a bonding intermediate to Si_3N_4 and Si_2NO [4, 17, 18]. The BE being about 0.6 eV higher than in Si_3N_4, it was attributed to a hydrogen/dangling bond [4]. Recent work [8] has indeed calculated a shift of 0.6 eV in the BE for a Si_2NH configuration. The small deviation (<10%) from the Mott rule, which requires $2x + 3y = 4$ for a SiO_xN_y film, is also suggestive of a small amount of hydrogen in the films [9].

Figure 3 shows the XPS valence band spectra for $SiO_{1.9}N_{0.1}$ and $SiO_{1.6}N_{0.3}$ obtained using a monochromatic Al Kα source. The N 2s feature centred at 19.2 eV BE shows increased intensity in $SiO_{1.6}N_{0.3}$ compared to $SiO_{1.9}N_{0.1}$, which exhibits only a very weak feature. The spectra in figure 3 are plotted with the O 2s peak intensity at 24.4 eV normalized taking into account the reduced oxygen content in $SiO_{1.6}N_{0.3}$ compared to $SiO_{1.9}N_{0.1}$. Note the absence of the C 2s peak expected [19] at a BE of 17.1 eV. The $SiO_{1.9}N_{0.1}$ valence band spectrum is, in fact, quite similar to the SiO_2 spectrum reported for a thermally grown oxide [9], except for the small tailing seen between 2 and 4 eV BE. This tailing is better seen in the $SiO_{1.6}N_{0.3}$ spectrum and is directly related to reduction of the band gap of amorphous Si_3N_4 (∼5.0 eV) compared to SiO_2 (∼9 eV; see [20]). The valence band spectra are very similar to those obtained from PECVD deposited SiO_xN_y films using Silane [9].

Figure 4 shows atomic concentrations as a function of depth obtained from an electron-induced AES depth profile, with etching time converted into depth. The composition is fairly uniform over the thickness of the deposited film. Similar profiles have been obtained over the area of films deposited on 125 mm pseudo-square solar cells. The mid-point of the crossover in Si and oxygen concentrations is the film thickness and gives a deposition rate of ∼60 Å min^{-1}. While this deposition rate is small, we could grow $SiO_{1.6}N_{0.3}$ films up to a thickness of 2700 Å at the same deposition rate. Having established the conditions for growing high-quality films using HMDSN and knowing the deposition rate and composition, films of thickness 870 ± 15 Å were grown as an AR coating for textured 125 mm pseudo-square Si solar cells[1]. A batch of 60 cells were tested for efficiency (AM 1) before and after deposition. The efficiency was determined from I–V plots, obtained with and without the AR coatings, which showed an increase in the operating current (I_{op}) under illumination. The increase in I_{op} is indicative of an effective surface passivation of the solar cells due to a reduction in interface state density. It is known that PECVD of SiO_2 or Si_3N_4 reduces interface state density resulting in the increase of output power and hence, efficiency [21]. The AM 1 efficiency in the present case increased from 12.0% to 13.1 ± 0.1% for the entire batch of solar cells.

In conclusion, SiO_xN_y films have been grown starting with an organic precursor (HMDSN) as a source of Si but which are carbon-free (<1%). XPS and AES are used to study and confirm the electronic structure of the films in agreement with films grown using silane. For a $\lambda/4$ 'blue' AR coating on solar cells with uniform thickness (870 ± 15 Å) and composition ($SiO_{1.6\pm0.1}N_{0.3\pm0.05}$), an efficiency increase of 1% is obtained.

[1] The composition $SiO_{1.6}N_{0.3}$ gives a refractive index of ∼1.7 [16]. Hence, a thickness of 850–880 Å serves as a $\lambda/4$ AR coating.

Acknowledgments

We thank Dr V Ramachandran, Dr S Ravi and Dr K P Raghunath for valuable discussions and the solar cell efficiency measurements. Partial financial support from BHEL, Electronics Division, is acknowledged.

References

[1] Lucovsky G and Phillips J C 2000 *Appl. Surf. Sci.* **166** 497
Lucovsky G, Wu Y, Niimi H, Misra V and Phillips J C 1999 *Appl. Phys. Lett.* **74** 2005
[2] Martinu L and Poitras D 2000 *J. Vac. Sci. Technol.* A **18** 2619
[3] Chang S-T, Johnson N M and Lyon S A 1984 *Appl. Phys. Lett.* **44** 318
Yang W, Jayaraman R and Sodini C G 1988 *IEEE Trans. Electron Devices* **35** 935
Ramesh K, Chandorkar A N and Vasi J 1989 *J. Appl. Phys.* **65** 3958
[4] Carr E C and Buhrman R A 1993 *Appl. Phys. Lett.* **63** 54
[5] Ellis K A and Buhrman R A 1996 *Appl. Phys. Lett.* **69** 535
[6] Bulkin P V, Swart P L and Lacquet B M 1995 *J. Non. Cryst. Solids* **187** 403
[7] Lu H C, Gusev E P, Gustafsson T, Garfunkel E, Green M L, Brasen D and Feldman L C 1996 *Appl. Phys. Lett.* **69** 2713

[8] Rignanese G M, Pasquarello A, Charlier J-C, Gonze X and Car R 1997 *Phys. Rev. Lett.* **79** 5174
Rignanese G M and Pasquarello A 2000 *Appl. Phys. Lett.* **76** 553
[9] Gritsenko V A, Xu J B, Kwok R W M, Ng Y H and Wilson I H 1998 *Phys. Rev. Lett.* **81** 1054
[10] Jeong S and Oshiyama A 2001 *Phys. Rev. Lett.* **86** 3574
[11] Inagaki N, Kondo S, Hirata M and Urushibata H 1985 *J. Appl. Polym. Sci.* **30** 3385
Bushnell-Watson S M, Alexander M R, Ameen A P, Rainforth W M, Short R D and Jones F R 1995 *The Mechanics of Thin Film Coatings* ed P H Gaskell, M D Savage and J L Summers (Singapore: World Scientific) p 377
[12] Ma Y and Lucovsky G 1994 *J. Vac. Sci. Technol.* B **12** 2504
[13] *Handbook of Auger Electron Spectroscopy* 1995 ed C L Hedberg (Minnesota: Physical Electronics)
Handbook of X-Ray Photoelectron Spectroscopy 1995 ed J Chostain and R C King (Minnesota: Physical Electronics)
[14] Wagner C D, Davis L E and Riggs W M 1980 The inelastic mean free path is 30 Å for Si 2p electrons *Surf. Int. Anal.* **2** 53
Iqbal A, Jackson W B, Tsai C C, Allen J W and Bates C W Jr 1987 *J. Appl. Phys.* **61** 2947
[15] Mcguire G E 1994 *Handbook of Deposition Technologies for Films and Coatings* ed R F Bunshah (New Jersey: Noyes) p 763
[16] Brytov I A, Gritsenko V A and Romashchenko Yu N 1985 *Sov. Phys. JETP* **62** 321
[17] Bischoff J L, Lutz F, Bolmont D and Kubler L 1991 *Surf. Sci.* **251/252** 170
[18] Hegde R I, Tobin P J, Reid K G, Maiti B and Ajuria S A 1995 *Appl. Phys. Lett.* **66** 2882
[19] Lapiano-Smith D A, Himpsel F J and Terminello L J 1993 *J. Appl. Phys.* **74** 5842
[20] Sze S M 1981 *Physics of Semiconductor Devices* (New York: Wiley) p 852
[21] Leguijt C *et al* 1996 *Solar Energy Mater. Solar Cells* **40** 297